Key role of subdaily wind variability for tropical surface wind stress

Yunwei Yan,[a,b] Xiangzhou Song,[a,b] Marilena Oltmanns,[c]

[a] *Key Laboratory of Marine Hazards Forecasting, Ministry of Natural Resources, Hohai University, Nanjing, China*

[b] *College of Oceanography, Hohai University, Nanjing, China*

[c] *National Oceanography Centre, Southampton, UK*

Corresponding author: Yunwei Yan, yunwei.yan@hhu.edu.cn

Early Online Release: This preliminary version has been accepted for publication in *Journal of Physical Oceanography*, may be fully cited, and has been assigned DOI 10.1175/JPO-D-22-0156.1. The final typeset copyedited article will replace the EOR at the above DOI when it is published.

ABSTRACT

High-frequency observations of surface winds over the open ocean are available only at limited locations. However, these observations are essential for assessing atmospheric influences on the ocean, validating reanalysis products, and building parameterization schemes. By analyzing high-frequency measurements from the Global Tropical Moored Buoy Array, the effects of subdaily winds on the mean surface wind stress magnitude are systematically examined. Subdaily winds account for 12.4% of the total stress magnitude on average. The contribution is enhanced over the Intertropical Convergence Zone and reaches a maximum (28.5%) in the equatorial western Pacific. The magnitude of the contribution is primarily determined by the kinetic energy of subdaily winds. Compared to the buoy observations, the ERA5 and MERRA2 subdaily winds underestimate this contribution by 51% and 63% due to underestimations of subdaily kinetic energy, leading to 7% and 8% underestimations in the total stress magnitude, respectively. Two new gustiness parameterization schemes related to precipitation are developed to account for the effect of subdaily winds, explaining ~80% of the contribution from subdaily winds. Considering the importance of wind stress for ocean-atmosphere interactions, the inclusion of these parametrization schemes in climate models is expected to substantially improve simulations of large-scale climate variability.

SIGNIFICANCE STATEMENT

Surface wind stress drives upper ocean circulation, which is critical for the redistribution of mass, momentum, and energy in the ocean. Moreover, it is one of the key factors controlling oceanic turbulent mixing and therefore has significant impacts on the distribution of temperature, salinity and associated ocean variability. Using high-resolution buoy observations, this study highlights the importance of subdaily winds for integrated wind stress estimates. In addition, it finds that current state-of-the-art and widely used reanalysis products largely underestimate the effect of subdaily winds. Two new parameterization schemes are developed, leading to a better representation of the effect of subdaily winds. Including the proposed parametrization schemes in climate models is expected to substantially improve their simulations of large-scale climate variability.

Accepted for publication in *Journal of Physical Oceanography*. DOI 10.1175/JPO-D-22-0156.1.

1. Introduction

Wind stress at the sea surface is the main driver of global ocean circulation, redistributing mass, momentum and energy in the ocean (e.g., Gill 1982; Wunsch and Ferrari 2004). Moreover, representing the momentum flux between the atmosphere and the ocean, surface wind stress is one of the key factors controlling oceanic turbulent mixing and therefore exerts significant impacts on ocean temperature and salinity (e.g., Ouni et al. 2021; Zhou et al. 2018). Due to the nonlinear dependence of wind stress on wind, the high-frequency variability of winds has a large influence on low-frequency wind stress (e.g., Ponte and Rosen 2004; Zhai et al. 2012). Many studies have shown that the synoptic variability in surface winds makes a significant contribution to the mean wind stress, with far-reaching implications for ocean circulation and turbulent mixing (e.g., Duteil 2019; Lin et al. 2018; 2020; Ponte and Rosen 2004; Wu et al. 2016; 2020; Zhai 2013; Zhai and Wunsch 2013; Zhai et al. 2012). For example, Duteil (2019) found that removing synoptic winds (2 days to 1 month) in the tropical Pacific decreased the mean wind stress by up to 20%, weakening the wind-driven ocean circulation by 20%.

Likewise, neglecting subdaily wind variability may have severe effects on mean wind stress estimates (e.g., Eymard et al. 2003; Ledvina et al. 1993; Ouni et al. 2021; Zhai et al. 2012; Zhou et al. 2018). Based on ship/buoy measurements during March and April 1998 in the northwestern Mediterranean Sea, Eymard et al. (2003) evaluated the impact of the subdaily variability of air-sea parameters on air-sea flux estimates. They found a strong underestimation of the mean momentum flux when the vector-averaged winds were employed; the mean friction velocity decreased by 22% (Table 3 in their paper). Due to the nonlinear effect, subdaily winds exert significant impacts on wind power input to the ocean and ocean temperature and salinity at longer timescales (e.g., Lee and Liu 2005; Ouni et al. 2021; Zhai et al. 2012; Zhou et al. 2018). Zhai et al. (2012) showed that including subdaily winds in analyses led to a one-third increase in the estimated total wind power input to the ocean through an increased mean wind stress (Table 1 in their paper). Zhou et al. (2018) conducted sensitivity experiments using a one-dimensional ocean model at 15.5°N, 61.5°E and found that including subdaily signals in the wind field lowered the daily mean sea surface temperature (SST) by 0.8°C on average, primarily due to intensified wind stress magnitude and turbulent heat fluxes.

Accepted for publication in *Journal of Physical Oceanography*. DOI 10.1175/JPO-D-22-0156.1.

To date, however, the contribution of subdaily winds to the mean wind stress has not been quantified on a global scale. The Global Tropical Moored Buoy Array (GTMBA) provides long-term high-frequency (10-minute and hourly) measurements of air-sea variables across the entirety of the tropical oceans (McPhaden et al. 2010), allowing us to address this problem. Buoy observations have been used to investigate some of the characteristics of subdaily winds, such as diurnal and semidiurnal cycles and wind gusts (e.g., Christophersen et al. 2020; Deser and Smith 1998; Giglio et al. 2017; 2022; Joseph et al. 2021; Serra et al. 2007; Turk et al. 2021; Ueyama and Deser 2008). Here, these data are used to investigate the relation between subdaily winds and the mean wind stress. Thus, the first objective of this paper is to systematically quantify the effects of subdaily winds on the mean wind stress magnitude across the entirety of the tropical oceans using GTMBA observations.

Given the importance of subdaily winds, their effect on the ocean has been taken into account in numerical simulations by employing wind forcing with subdaily variability (e.g., Ouni et al. 2021; Thushara and Vinayachandran 2014; Yu et al. 2020). Wind forcing with subdaily variability is largely available from the most recent atmospheric reanalysis products with hourly temporal resolutions, such as the 5th-generation ECMWF reanalysis product (ERA5, Hersbach et al. 2020) and the Modern-Era Retrospective analysis for Research and Applications product, Version 2 (MERRA2, Gelaro et al. 2017). However, the accuracy of subdaily winds in these reanalysis products is still unknown. Thus, the second objective of this paper is to evaluate the effect of subdaily winds on the mean wind stress magnitude in the ERA5 and MERRA2 reanalysis products.

A more efficient and less expensive approach to account for subdaily winds is to parameterize them by using a gustiness correction for the daily vector-averaged wind speed (e.g., Cronin et al. 2006; Praveen Kumar et al. 2012; 2013). For example, Praveen Kumar et al. (2012) proposed a climatological gustiness parameterization scheme related to SST and applied the gustiness correction to account for unresolved subdaily winds in the TropFLUX reanalysis product. An evaluation showed that including the gustiness correction increased the mean wind stress magnitude by ~5% (Fig. 2d in Praveen Kumar et al. 2013). In this study, we relate gustiness to the precipitation rate, which has a close relation to the momentum flux associated with subdaily winds (see Section 3). Two new gustiness

Accepted for publication in *Journal of Physical Oceanography*. DOI 10.1175/JPO-D-22-0156.1.

parameterization schemes are proposed: one is time-independent, similar to that of Praveen Kumar et al. (2012), and the other is time dependent. This is the third objective of this study.

This paper is structured as follows: After a short description of the data and methods in Section 2, Section 3 will present the major results of this study. First, the contribution of subdaily winds to the mean wind stress magnitude is estimated from the GTMBA observations, and then the effects of subdaily winds in the ERA5 and MERRA2 products are evaluated. Finally, two new parameterization schemes to represent unresolved subdaily winds are developed. Conclusions are drawn in Section 4.

2. Data and Methods

To estimate air-sea fluxes, the GTMBA observations are used as inputs for the Coupled Ocean-Atmosphere Response Experiment (COARE) 3.5 bulk flux algorithm (Edson et al. 2013). The GTMBA observations provide long-term, high-frequency measurements (10-minute and hourly) of air-sea variables, including surface vector winds, surface air temperature and relative humidity, and water temperature near the surface (McPhaden et al. 2010). The 10-minute measurements were averaged into hourly means before the flux estimate. For surface winds, we used vector averaging. More information about the GTMBA observations was provided in Yan et al. (2021, 2022).

The wind stress magnitude (τ) is estimated using the COARE 3.5 bulk flux algorithm (Edson et al. 2013):

$$\tau = \rho \cdot C_d(|\boldsymbol{V}|) \cdot |\boldsymbol{V}| \cdot S = \rho \cdot C_d(|\boldsymbol{V}|) \cdot |\boldsymbol{V}|^2 \cdot f_G \qquad (1)$$

where ρ is the near-surface air density, C_d is the drag coefficient, $\boldsymbol{V}$ is the hourly vector-averaged surface winds, $|\boldsymbol{V}|$ is the vector-averaged wind speed ($|\boldsymbol{V}| = \sqrt{u^2 + v^2}$, where u and v are the zonal and meridional components of the hourly vector-averaged surface winds), S is the hourly scalar-averaged wind speed, and f_G is the convective gustiness factor ($f_G = S/|\boldsymbol{V}|$, representing the ratio of the hourly scalar-averaged wind speed to the vector-averaged wind speed). The factor attempts to eliminate the estimation error when the vector-averaged winds approach zero, but the scalar-averaged wind speed is nonzero (Fairall et al. 1996). The drag coefficient is dependent on wind speed and atmospheric stability. Here, for convenience, the drag coefficient is expressed as a function of wind speed only. The true wind speed, rather

Accepted for publication in *Journal of Physical Oceanography*. DOI 10.1175/JPO-D-22-0156.1.

than the relative wind speed, is used due to the lack of credible data on tropical surface currents with a diurnal jet (Masich et al. 2021).

Next, the wind stress magnitude induced by the mean daily wind vector is calculated using the COARE 3.5 algorithm ($\tau\_MDW = \rho \cdot C_d(|\overline{\boldsymbol{V}}|) \cdot |\overline{\boldsymbol{V}}|^2 \cdot f_G$, where $\overline{\boldsymbol{V}}$ is the mean daily wind vector). The difference between τ and τ_MDW is defined as the wind stress magnitude induced by subdaily winds (τ_SDW). The annual climatology of τ_SDW is obtained by averaging all available samples to represent the effects of subdaily winds on the mean wind stress magnitude. Only buoys with more than two years of available data are selected in this study. Note that convective gustiness is also considered in the estimation of τ_MDW. Therefore, the nominal subdaily winds in this study represent winds at timescales between 1 day and 1 hour.

To examine how subdaily winds influence the mean wind stress magnitude, the variables in Equation (1) are divided into two components:

$$C_d(|\boldsymbol{V}|) = \overline{C_d(|\boldsymbol{V}|)} + C_d(|\boldsymbol{V}|)'$$

$$|\boldsymbol{V}| = \overline{|\boldsymbol{V}|} + |\boldsymbol{V}|' \qquad (2)$$

where an overbar denotes the daily mean and a prime symbol denotes a subdaily fluctuation. The contribution of subdaily winds to the daily mean wind stress magnitude ($\overline{\tau\_SDW}$) is written as

$$\overline{\tau\_SDW} = \bar{\tau} - \overline{\tau\_MDW}$$

$$= \underbrace{\rho \cdot f_G \cdot \overline{C_d(|\boldsymbol{V}|)} \cdot (\overline{|\boldsymbol{V}|^2} - |\overline{\boldsymbol{V}}|^2)}_{mean\ wind\ speed\ change\ term} + \underbrace{\rho \cdot f_G \cdot [\overline{C_d(|\boldsymbol{V}|)} - \overline{C_d(|\overline{\boldsymbol{V}}|)}] \cdot |\overline{\boldsymbol{V}}|^2}_{mean\ drag\ coefficient\ change\ term}$$

$$+ \underbrace{\rho \cdot f_G \cdot \overline{C_d(|\boldsymbol{V}|) \cdot |\boldsymbol{V}|'^2}}_{wind\ speed\ variance\ term} + \underbrace{2 \cdot \rho \cdot f_G \cdot \overline{|\boldsymbol{V}|} \cdot \overline{C_d(|\boldsymbol{V}|)' \cdot |\boldsymbol{V}|'}}_{covariance\ term} \qquad (3)$$

Here, the convective gustiness factor for estimating wind stress associated with the mean daily wind vector (τ_MDW) is assumed to be equal to that in the estimation of the hourly wind stress (τ). This assumption leads to a 3% increase in the total contribution of subdaily winds. The terms on the right-hand side of Equation (3) represent the contributions from changes in the mean wind speed and drag coefficient, wind speed variance, and covariance between wind speed and drag coefficient due to subdaily winds. Here, these terms are defined

Accepted for publication in *Journal of Physical Oceanography*. DOI 10.1175/JPO-D-22-0156.1.

as the mean wind speed change (MWSC) term, mean drag coefficient change (MDCC) term, wind speed variance (WSV) term, and covariance (CV) term. The annual climatologies of all the terms are calculated using the GTMBA observations to assess their corresponding effects on the mean wind stress magnitude.

Likewise, all the terms in Equation (3) are estimated using the hourly ERA5 and MERRA2 reanalysis wind values to evaluate their performance. Note that the wind stresses estimated from ERA5 and MERRA2 are based on the COARE algorithm for the convenience of comparison with those derived from the GTMBA observations. However, wind stresses directly downloaded from these two reanalyses are estimated using their own algorithms. For example, the ERA5 air-sea fluxes are calculated using the ECMWF algorithm (ECMWF, 2021). Therefore, the wind stress magnitudes of the reanalysis products in this study refer to our calculated wind stresses via the COARE algorithm.

Finally, we develop two new parameterization schemes to account for the effect of subdaily winds: one is time dependent, and the other is not. We use the gustiness approach, which has been widely applied to parameterize unresolved wind variability at different spatial and temporal scales (e.g., Bessac et al. 2019; 2021; Blein et al. 2020; 2022; Godfrey and Beljaars 1991; Hourdin et al. 2020; Redelsperger et al. 2000; Zeng et al. 2002). To establish the time-independent scheme, the climatological gustiness value (G_{clim}) is first calculated from the GTMBA observations per the methods of Cronin et al. (2006): $G_{clim} = \sqrt{\langle|\overline{V}|^2 - |\bar{V}|^2\rangle}$, where an angle bracket denotes a record-length average at each buoy site. The gustiness value (G_{clim}) was defined as the mesoscale gustiness, representing the impact of subdaily winds (at timescales between 1 day and 1 hour) on wind speed (Cronin et al. 2006). It is nearly twice as large as the convective gustiness in the equatorial eastern Pacific Ocean (Cronin et al. 2006). Next, a simple linear function is built between the square of the gustiness value (G_{clim}^2) and the corresponding precipitation rate (P_{clim}). Here, we select G_{clim}^2, rather than G_{clim}, to build the regression model due to the quadratic relation between wind stress magnitude and wind speed (Equation 1). Likewise, the time-dependent scheme using monthly values is created based on the expression of the Michaels-Menten equation. We also apply the Michaels-Menten equation to build the time-independent scheme, and it performs as well as the linear model. For simplicity, only the linear regression model is given

Accepted for publication in *Journal of Physical Oceanography*. DOI 10.1175/JPO-D-22-0156.1.

for the time-independent scheme in this study. The precipitation rate used here is the research-level product of the Integrated MultisatellitE Retrievals for GPM (IMERG Final Run).

3. Results

We start by examining the mean surface wind stress magnitude obtained from the GTMBA observations (Fig. 1a). Spatially, the wind stress magnitude is relatively small in the calm equatorial belt, especially in the equatorial Indian Ocean, western Pacific and equatorial cold tongue region of the Pacific and Atlantic, reaching amplitudes of less than 4×10^{-2} N/m^2. In contrast, the wind stress magnitude is larger in areas farther from the equator, such as the trade winds region, where it reaches amplitudes of over 8×10^{-2} N/m^2. Subdaily winds make a positive contribution to the mean wind stress magnitude (Figs. 1b-1c), with an average contribution of 6.5×10^{-3} N/m^2 (12.4%) in the tropics. The contribution is particularly large over the Intertropical Convergence Zone (ITCZ), a region characterized by strong precipitation, and it increases to 8.4×10^{-3} N/m^2 (17.4%) in regions with a surface precipitation rate greater than 5 mm/day. The maximum percentage contribution from subdaily winds reaches 28.5% in the equatorial western Pacific, where the mean wind stress magnitude is small. The estimates from buoy observations suggest that subdaily winds have a nonnegligible effect on the mean surface wind stress magnitude over the tropics, especially over the ITCZ.

Accepted for publication in *Journal of Physical Oceanography*. DOI 10.1175/JPO-D-22-0156.1.

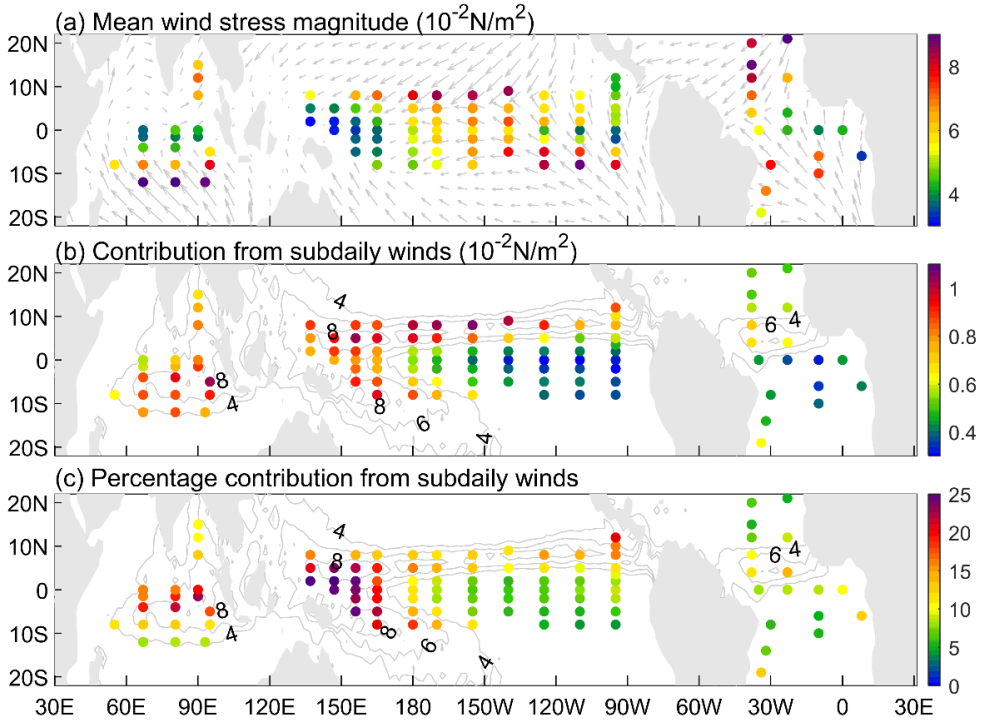

Fig. 1. (a) Mean surface wind stress magnitude estimated from GTMBA observations. (b, c) Contribution from subdaily winds to the mean wind stress magnitude and the corresponding percentage. Gray arrows and contours denote the satellite-derived mean surface wind stress (a) and precipitation rate (mm/day, b, c), respectively. The satellite-derived mean wind stress was calculated from the Scatterometer Climatology of Ocean Winds (SCOW, Risien and Chelton, 2008).

The contribution from subdaily winds to the mean wind stress magnitude arises from four aspects, which are associated with the mean wind speed change, mean drag coefficient change, wind speed variance, and covariance between wind speed and the drag coefficient (see Equation 3). The MWSC, MDCC, WSV, and CV terms are all estimated from the GTMBA observations and amount to 3.5×10^{-3}, 0.8×10^{-3}, 2.1×10^{-3}, and 0.4×10^{-3} N/m^2 (51.9%, 12.3%, 31.2%, and 7.8%), respectively, on average, using all buoy sites (Fig. 2). The two largest contributors are associated with the MWSC and WSV terms, which account for approximately 80% of the overall contribution. The other two terms, which are related to the variable drag coefficient, make an approximately 20% total contribution. Moreover, the

Accepted for publication in *Journal of Physical Oceanography*. DOI 10.1175/JPO-D-22-0156.1.

MWSC and WSV terms exhibit significant spatial variations, with large values located over the ITCZ, while the spatial distributions of the other two terms are relatively uniform (see also Fig. S1). The enhanced MWSC and WSV terms over the ITCZ are thus the main contributors to the increased wind stress magnitude in these regions. The spatial correlation coefficient between the MWSC (WSV) term and the total contribution is 0.98 (0.93). This result implies that the contribution from subdaily winds to the mean wind stress magnitude largely results from the MWSC and WSV terms, which are related to the change in the mean wind speed due to subdaily winds and the variance in subdaily wind speed variability.

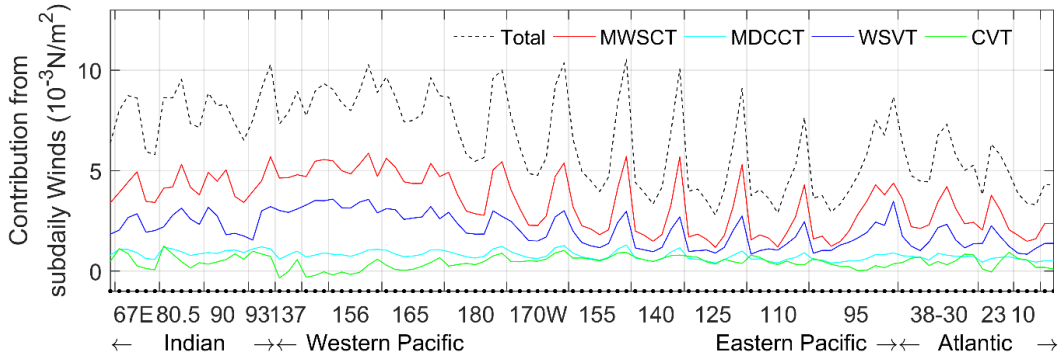

Fig. 2. All the terms in Equation (3) estimated from the GTMBA observations: The total contribution (black curve, representing the values at all buoy sites as shown in Fig. 1b but ordered from west to the east and from south to north; the order is listed in Table S1; black dots on the x-axis denote the buoys, and the corresponding labels are their longitudes), mean wind speed change term (red curve), mean drag coefficient change term (cyan curve), wind speed variance term (blue curve), and covariance term (green curve).

Having calculated the contribution of subdaily winds to the mean wind stress, we next investigate the total change in wind speed, averaged over the full record, that results from the subdaily winds ($\langle \overline{|V|} - |\bar{V}| \rangle$, Fig. 3a). The mean wind speed increases over the entire tropical region, with the increase being enhanced over the ITCZ. Specifically, the average value of the increase is 0.29 m/s in the tropics and rises to 0.41 m/s over the ITCZ (surface precipitation rate > 5 mm/day). The variance in the subdaily wind speed variability ($\langle |V|'^2 \rangle$) exhibits a similar spatial structure, with large values located over the ITCZ (1.35 m^2/s^2, Fig. 3b). The enhanced mean wind speed change (subdaily wind speed variance) over the ITCZ

Accepted for publication in *Journal of Physical Oceanography*. DOI 10.1175/JPO-D-22-0156.1.

leads to the increase in the MWSC (WSV) term in these regions, indicated by a high correlation coefficient of 0.95 (0.99) between them.

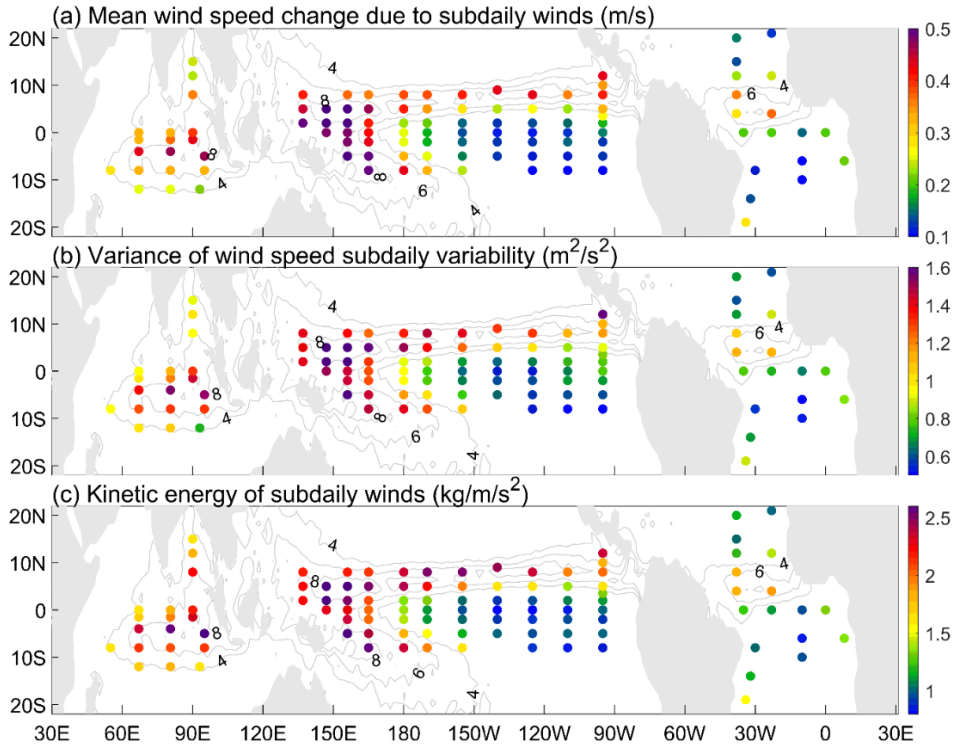

Fig. 3. (a) Change in the mean wind speed due to subdaily winds ($\langle|\overline{V}| - |\bar{V}|\rangle$). (b) Variance in subdaily wind speed variability ($\langle|\boldsymbol{V}|'^2\rangle$). (c) Kinetic energy of subdaily winds ($\langle\rho \cdot (u'^2 + v'^2)\rangle/2$). Gray contours in (a-c) denote the satellite-derived mean surface precipitation rate (mm/day).

Considering that the mean wind speed change and subdaily wind speed variance are both dependent on the strength of subdaily winds, the kinetic energy of subdaily winds is examined next. The kinetic energy is calculated as $\langle\rho \cdot (u'^2 + v'^2)\rangle/2$, where u' and v' are the zonal and meridional components of subdaily winds. It is evident that the subdaily winds are strong over the ITCZ, which is characterized by high kinetic energy (Fig. 3c). The strong subdaily winds over the ITCZ induce large mean wind speed changes and subdaily wind speed variances, resulting in large subdaily wind contributions. Additionally, there is a linear

Accepted for publication in *Journal of Physical Oceanography*. DOI 10.1175/JPO-D-22-0156.1.

relationship between the subdaily wind contribution ($\langle \tau\_SDW \rangle$, units: 10^{-3} N/m^2) and the kinetic energy of subdaily winds ($\langle KE\_SDW \rangle$, units: kg/m/s^2):

$$\langle \tau\_SDW \rangle = 3.554 \cdot \langle KE\_SDW \rangle + 0.58 \qquad (4)$$

where the explained variance (determination coefficient) is 0.93 and the root mean square error (RMSE) is 0.57 (Fig. 4). The linear relationship can be derived from the formula for the mean wind stress magnitude from subdaily winds, assuming constant convective gustiness and drag coefficient:

$$\overline{\tau\_SDW} = \rho \cdot C_d \cdot \left(\overline{u^2 + v^2}\right) \cdot f_G - \rho \cdot C_d \cdot (\bar{u}^2 + \bar{v}^2) \cdot f_G = 2 \cdot f_G \cdot C_d \cdot \overline{KE\_SDW} \qquad (5)$$

The linear expression can also be obtained from equation (3) (not shown). Thus, the contribution of subdaily winds to the mean wind stress magnitude primarily depends on the kinetic energy (strength) of the subdaily winds. The high kinetic energy over the ITCZ may be associated with the frequently occurring mesoscale convective system there (e.g., Yuan and Houze 2010; Feng et al. 2021), which can enhance the subdaily winds by generating cold pools (density currents) at the sea surface (e.g., Garg et al. 2021; Joseph et al. 2021). Future analyses quantifying the physical processes responsible for subdaily winds are desirable.

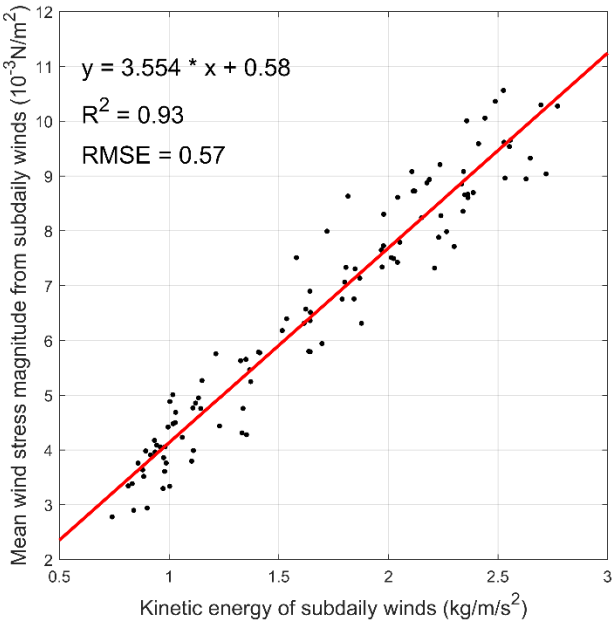

Fig. 4. Linear relationship between the mean wind stress magnitude from subdaily winds and the kinetic energy of subdaily winds.

Accepted for publication in *Journal of Physical Oceanography*. DOI 10.1175/JPO-D-22-0156.1.

To evaluate the role of the subdaily winds in the most recent atmospheric reanalysis products, the contribution from the subdaily winds to the mean wind stress magnitude is calculated from ERA5 and MERRA2 data. Notably, both products underestimate the contribution of subdaily winds (Fig. 5a). The mean absolute percentage error (MAE) in the tropics is 51% and 63% for ERA5 and MERRA2, respectively, where $MAE = |(reanalysis - observation)/observation| \times 100\%$. The value of the error in the contribution corresponds to the errors for the MWSC and WSV terms (the two largest contributors), which are underestimated by 50% and 49% (61% and 64%) in the ERA5 (MERRA2) product (Figs. 5b-5c). The underestimated MWSC and WSV terms in these two products arise from the underestimations of the mean wind speed change due to subdaily winds (the MAEs are 47% and 59%) and the variance in subdaily wind speed variability (the MAEs are 56% and 71%), which are associated with the underestimation of the (strength) kinetic energy of subdaily winds (the MAEs are 59% and 72%, Fig. 5d).

Accepted for publication in *Journal of Physical Oceanography*. DOI 10.1175/JPO-D-22-0156.1.

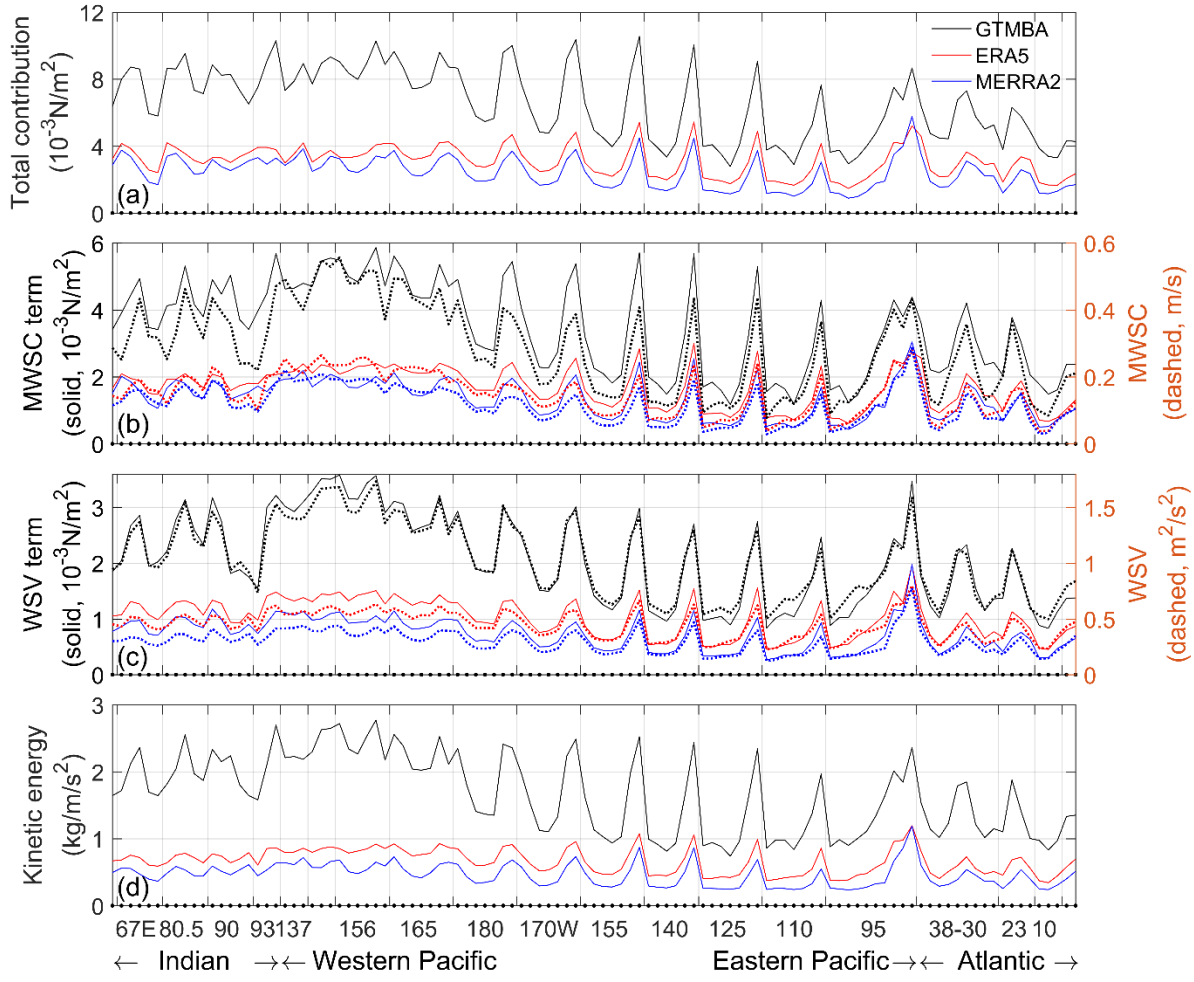

Fig. 5. (a) Contribution from subdaily winds to the mean wind stress magnitude at all buoy sites. (b) Change in the mean wind speed due to subdaily winds (dashed curve) and the associated contribution (solid curve). (c) Variance in subdaily wind speed variability (dashed curve) and the associated contribution (solid curve). (d) Kinetic energy of subdaily winds. Black, red, and blue curves denote values estimated from the GTMBA observations, ERA5 product and MERRA2 product, respectively. The X-axes in (a-d) are the same as those in Fig. 2.

To assess in more detail the extent to which ERA5 and MERRA2 products underestimate the effects of subdaily winds relative to the GTMBA observations, we next examine the kinetic energy spectrum of winds. The kinetic energy spectrum is calculated by averaging the zonal and meridional wind power spectra, which are obtained using Welch's overlapped

Accepted for publication in *Journal of Physical Oceanography*. DOI 10.1175/JPO-D-22-0156.1.

segment averaging estimator with a 60-day Hamming window and 0% overlap. The results include peaks at diurnal (24-hour) and semidiurnal (12-hour) timescales (Fig. 6), which have been reported in previous studies (Deser and Smith 1998; Ueyama and Deser 2008). The corresponding diurnal and semidiurnal winds are induced by atmospheric tides and/or land–sea breezes (Christophersen et al. 2020; Takahashi 2012; Ueyama and Deser 2008). ERA5 and MERRA2 are capable of reproducing diurnal (84% and 77%) and semidiurnal (111% and 91%) winds. However, at other subdaily timescales, these two reanalysis products underestimate wind variability, and the estimation performance decreases as the timescale becomes shorter. For example, the MAE of kinetic energy is 48% (55%) between the 24-hour and 23-hour timescales and increases to approximately 94% (100%) between the 3-hour and 2-hour timescales in the ERA5 (MERRA2) product. The underestimation of the kinetic energy at these timescales results in underestimated subdaily winds in the ERA5 and MERRA2 products. A reason for the underestimated kinetic energy in atmospheric reanalyses is that, in numerical models, the energy in the highest resolved wavenumbers is damped due to the nature of numerical solutions and parameterizations (Abdalla et al. 2013; Bolgiani et al. 2022; Klaver et al. 2020; Skamarock 2004). The model's effective resolution is typically 7 times the model grid spacing (Skamarock 2004). Recently, Bolgiani et al. (2022) showed that ERA5 has an effective resolution of 1300 to 1100 km in the tropical band and hence does not adequately capture mesoscale variability. In contrast, the buoy observations at fixed points reflect the contributions due to mesoscale spatial variability.

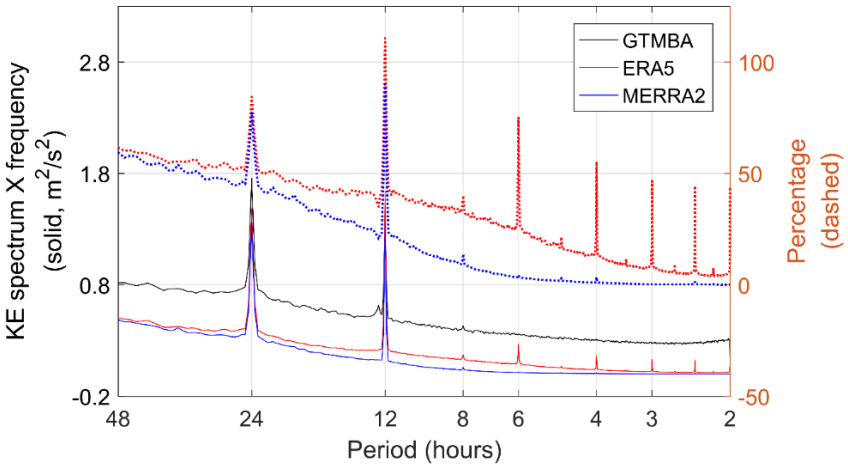

Fig. 6. Kinetic energy spectrum of surface winds (variance-preserving plots, solid curve) and the ratio between the reanalysis estimates and observations (percentage, dashed curve).

Accepted for publication in *Journal of Physical Oceanography*. DOI 10.1175/JPO-D-22-0156.1.

Black, red, and blue curves denote values estimated from the GTMBA observations, ERA5 product and MERRA2 product, respectively.

Importantly, the underestimated contribution from the ERA5 (MERRA2) subdaily winds results in a 7% (8%) error in the mean wind stress magnitude, on average, in the tropics (black curve in Fig. 7). The error increases to 12% (14%) in the tropical western Pacific. The total underestimation of the mean wind stress magnitude is 11% (18%) in the ERA5 (MERRA2) product based on GTMBA observations (red curve in Fig. 7). The underestimation of the subdaily wind contribution accounts for 60% (44%) of the total error in the mean ERA5 (MERRA2) wind stress magnitude. This percentage ratio rises to 73% (88%) in the tropical western Pacific, implying that accurate simulations of subdaily winds in ERA5 and MERRA2 will greatly improve estimates of the mean wind stress magnitude in the tropics, especially in the tropical western Pacific.

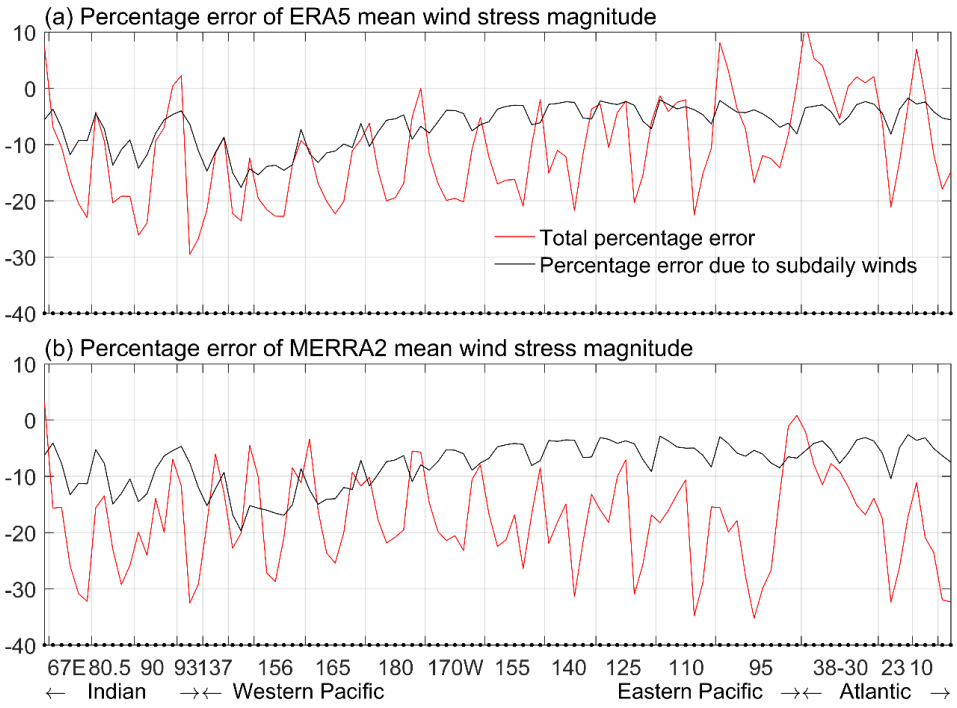

Fig. 7. Percentage error (red curve) of the mean wind stress magnitude in the ERA5 (a) and MERRA2 (b) products based on the GTMBA observations. The black curve denotes the percentage relative error associated with inaccurate subdaily winds. The X-axes are the same as those in Fig. 2.

Accepted for publication in *Journal of Physical Oceanography*. DOI 10.1175/JPO-D-22-0156.1.

The preceding analysis shows that two state-of-the-art reanalysis products largely underestimate the impact of subdaily winds, suggesting potential biases in ocean numerical simulations. We therefore develop a gustiness parameterization scheme to properly represent the effect of subdaily winds. Two new schemes are proposed in this study: one is time dependent, and the other is not. Due to the close relation between flux enhancement and precipitation (Fig. 1b), these two schemes are parameterized with the precipitation rate. The detailed procedures can be seen in Section 2. The linear regression model for the time-independent scheme is expressed as:

$$G_{clim}^2 = 0.37 \cdot P_{clim} + 1.78 \qquad (6)$$

where the explained variance is 0.93 and the RMSE is 0.37 (Fig. 8). Applying the new gustiness correction to account for subdaily winds ($\tau\_G_{clim} = \rho \cdot C_d(|\bar{V}|) \cdot G_{clim}^2$) increases the mean wind stress magnitude by 9.6% at the GTMBA sites, which explains 81.0% of the contribution of subdaily winds. Compared with the climatological parametrization scheme based on SST by Praveen Kumar et al. (2012; 2013), the new scheme performs better. An ~20% underestimation of the subdaily wind contribution remains due to the use of invariable gustiness in the new scheme.

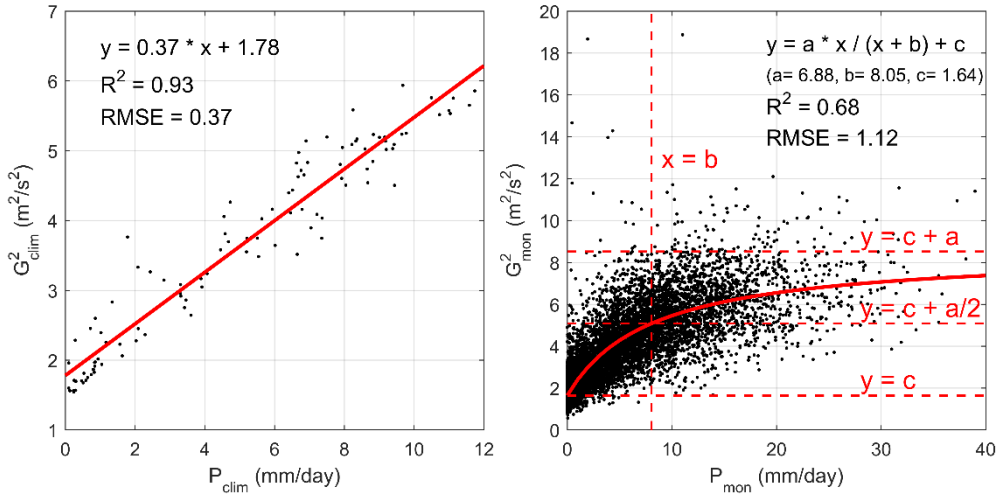

Fig. 8. Regression model between the square of the gustiness value (G^2) and precipitation rate (P) for the time-independent (left panel) and time-dependent (right panel) schemes.

Accepted for publication in *Journal of Physical Oceanography*. DOI 10.1175/JPO-D-22-0156.1.

To overcome the limitation of the time-independent scheme, a time-dependent scheme using monthly gustiness and precipitation (G_{mon} and P_{mon}) is built based on the following regression model:

$$G_{mon}^2 = \frac{a \cdot P_{mon}}{P_{mon} + b} + c \quad (7)$$

where a=6.88, b=8.05, and c=1.64. As shown in Fig. 8, the constant c represents the gustiness correction when there is no precipitation, a represents the maximum correction associated with precipitation, and b represents the precipitation rate corresponding to the half-maximum value of the precipitation-induced gustiness ($a/2$). The explained variance of the model is 0.68, and the RMSE is 1.12. Applying the time-dependent scheme explains 78.9% of the contribution of subdaily winds to the mean wind stress magnitude. The scheme has almost the same performance as the time-independent scheme. Including temporal variability does not improve the scheme performance because the relation between gustiness and precipitation becomes weaker at this timescale, as indicated by the explained variance of equation (7). We also tested a parameterization scheme based on wind speed, but the performance was lower than that of the scheme with precipitation. Thus, we have not included it here.

4. Conclusions and Discussion

Previous studies suggested that subdaily winds may contribute significantly to the mean surface wind stress, but direct estimates over the open ocean are lacking, and to date, there is no quantification of this contribution on a global scale. Here, the effects of subdaily winds on the mean surface wind stress magnitude were systematically quantified in the entirety of the tropical oceans using high-frequency measurements of air-sea variables from the GTMBA. We found that subdaily winds contribute 12.4% to the mean wind stress magnitude on average, and the contribution is large over the ITCZ. The magnitude of the contribution is primarily determined by the kinetic energy of subdaily winds. We also estimated the effect of subdaily winds on the mean wind stress vector (Fig. 9). The inclusion of subdaily winds clearly significantly enhances the mean stress vector. The zonal and meridional components increase by 3.2% and 9.4%, respectively. This suggests that including subdaily winds in

Accepted for publication in *Journal of Physical Oceanography*. DOI 10.1175/JPO-D-22-0156.1.

climate models would improve their simulations of the equatorial current regime and the resultant simulated ocean variability.

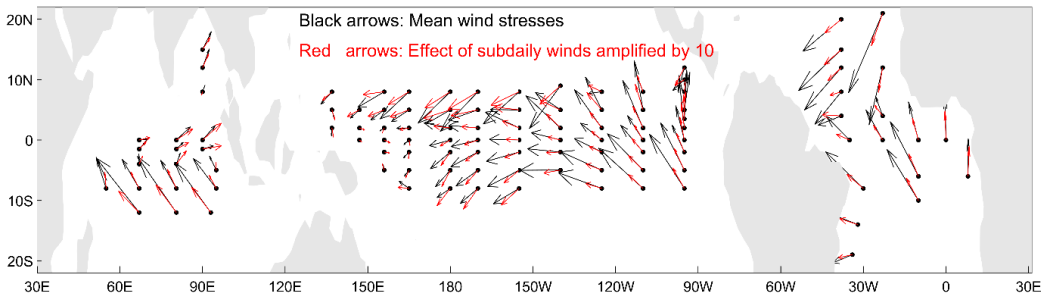

Fig. 9. Effect of subdaily winds on wind stress vector (red arrows). Black arrows denote the long-term mean wind stress vector. Red arrows are amplified by 10.

Thus, our study highlights the importance of subdaily winds for the total air-sea momentum flux in the tropics. Two state-of-the-art and widely used reanalyses, ERA5 and MERRA2, largely underestimate this effect by 51% and 63%, leading to 7% and 8% underestimations in the mean wind stress magnitude. Considering the importance of accurate wind stress estimates for simulating air-sea interactions, the identified biases are expected to have far-reaching implications for the simulated ocean and climate variability in models. Notably, the wind stresses derived from ERA5 and MERRA2 use the COARE algorithm, rather than their own bulk algorithms. To investigate the sensitivity to different algorithms, we also employ the ERA5 own algorithm (ECMWF algorithm) to estimate the effect of ERA5 subdaily winds. The estimated contribution of subdaily winds using the ECMWF algorithm is almost the same as that using the COARE algorithm (Figure 10a). This finding suggests that our main conclusions are insensitive to the bulk algorithm. It is worth to mention that the ECMWF algorithm slightly overestimates the contribution of the ERA5 subdaily winds with respect to the COARE algorithm (Figure 10). The bulk formula (Equation 1) shows that the discrepancy between different bulk algorithms for estimating wind stress mainly relies on the parameterizations for drag coefficient and convective gustiness. The parameterizations for convective gustiness are the same in the COARE and ECWMF algorithms (Brodeau et al. 2017, also see black curve in Figure 10b). Therefore, the discrepancy results from the different parameterizations for drag coefficient typically differ

Accepted for publication in *Journal of Physical Oceanography*. DOI 10.1175/JPO-D-22-0156.1.

by approximately 15% between the bulk algorithms (blue curve in Figure 10b; Bonino et al. 2022; Brodeau et al. 2017).

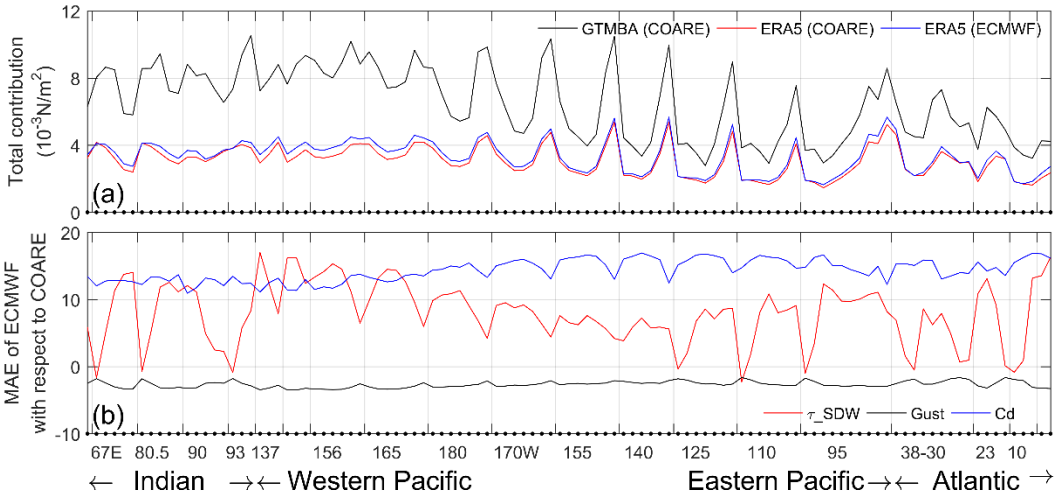

Fig. 10. (a) Contribution from subdaily winds to the mean wind stress magnitude estimated from the GTMBA observation using the COARE algorithm (black curve) and from the ERA5 reanalysis using the COARE (red curve) and ECMWF (blue curve) algorithms. (b) Mean absolute percentage errors of the subdaily wind contribution (red curve), convective gustiness (black curve) and drag coefficient (blue curve) calculated using the ECMWF algorithm with respect to those calculated using the COARE algorithm.

To improve the representation of subdaily winds, two parametrization schemes related to precipitation were developed in this study: one is time dependent, and the other is not. These two new schemes have almost the same performance regarding the effect of subdaily winds, explaining ~80% of the mean wind stress magnitude associated with subdaily winds. The inclusion of these parametrization schemes in climate models is expected to substantially improve simulations of large-scale climate variability. Note that there still exists an ~20% underestimation of the subdaily wind contribution when using these two schemes. Further improvements may potentially be achieved by future analyses that develop schemes based on different variables and techniques, for instance, using machine learning approaches. However, these analyses are beyond the scope of this study.

Accepted for publication in *Journal of Physical Oceanography*. DOI 10.1175/JPO-D-22-0156.1.

Acknowledgments.

This work is supported by the National Natural Science Foundation of China (41976028, 42122040, and 42076016).

Data Availability Statement.

The GTMBA measurements are available at https://www.pmel.noaa.gov/tao/drupal/disdel/, the ERA5 reanalysis at https://www.ecmwf.int/en/forecasts/datasets/reanalysis-datasets/era5, the MERRA2 reanalysis at https://disc.gsfc.nasa.gov/datasets?project=MERRA-2, and the IMERG products at https://gpm.nasa.gov/data/directory.

REFERENCES

Abdalla, S., L. Isaksen, P. Janssen, and N. Wedi, 2013: Effective spectral resolution of ECMWF atmospheric forecast models. ECMWF Newsletter, 137, 19-22, Available at: https://www.ecmwf.int/node/17358.

Bessac, J., A. H. Monahan, H. M. Christensen, and N. Weitzel, 2019: Stochastic parameterization of subgrid-scale velocity enhancement of sea surface fluxes. *Monthly Weather Review*, **147**(5), 1447-1469, doi:10.1175/MWR-D-18-0384.1.

Bessac, J., H. M. Christensen, K. Endo, A. H. Monahan, and N. Weitzel, 2021: Scale-aware space-time stochastic parameterization of subgrid-scale velocity enhancement of sea surface fluxes. *Journal of Advances in Modeling Earth Systems*, **13**, e2020MS002367, https://doi.org/10.1029/2020MS002367.

Blein, S., R. Roehrig, and A. Voldoire, 2022: Parameterizing the meso-scale enhancement of oceanic surface turbulent fluxes: a physical-statistical approach. *Quarterly Journal of the Royal Meteorological Society*, **148**, 1683-1708, doi:10.1002/qj.4273.

Blein, S., R. Roehrig, A. Voldoire, and G. Faure, 2020: Meso-scale contribution to air-sea turbulent fluxes at GCM scale. *Quarterly Journal of the Royal Meteorological Society*, **146**(730), 2466-2495, doi:10.1002/qj.3804.

Accepted for publication in *Journal of Physical Oceanography*. DOI 10.1175/JPO-D-22-0156.1.

Bolgiani, P., C. Calvo-Sancho, J. Díaz-Fernández, L. Quitián‐Hernández, M. Sastre, D. Santos‐Muñoz, J. I. Farrán, J. J. González‐Alemán, F. Valero, M. L. Martín, 2022: Wind kinetic energy climatology and effective resolution for the ERA5 reanalysis. *Clim Dyn* **59**, 737-752, https://doi.org/10.1007/s00382-022-06154-y.

Bonino, G., D. Iovino, L. Brodeau, and S. Masina, 2022: The bulk parameterizations of turbulent air–sea fluxes in NEMO4: the origin of sea surface temperature differences in a global model study. *Geoscientific Model Development*, 15, 6873-6889, https://doi.org/10.5194/gmd-15-6873-2022.

Brodeau, L., B. Barnier, S. K. Gulev, and C. Woods, 2017: Climatologically significant effects of some approximations in the bulk parameterizations of turbulent air–sea fluxes. *Journal of Physical Oceanography*, 47, 5-28, https://doi.org/10.1175/JPO-D-16-0169.1.

Christophersen, J. A., G. R. Foltz, and R. C. Perez, 2020: Surface Expressions of Atmospheric Thermal Tides in the Tropical Atlantic and Their Impact on Open-Ocean Precipitation. *Journal of Geophysical Research*, **125**, e2019JD031997, doi:10.1029/2019JD031997.

Cronin, M. F., C. W. Fairall, and M. J. McPhaden, 2006: An assessment of buoy-derived and numerical weather prediction surface heat fluxes in the tropical Pacific. *Journal of Geophysical Research*, **111**(C6), C06038, doi:10.1029/2005JC003324.

Deser, C., and C. A. Smith, 1998: Diurnal and semidiurnal variations of the surface wind field over the tropical Pacific Ocean. *Journal of Climate*, **11**(7), 1730-1748, doi:10.1175/1520-0442(1998)011<1730:DASVOT>2.0.CO;2.

Duteil, O., 2019: Wind synoptic activity increases oxygen levels in the tropical Pacific Ocean. *Geophysical Research Letters*, **46**(5), 2715-2725, doi:10.1029/2018GL081041.

ECMWF, 2021: IFS Documentation Cy47R3. Part IV: Physical Processes. Operational implementation 12 October 2021.

Edson, J. B., and Coauthors, 2013: On the exchange of momentum over the open ocean. *Journal of Physical Oceanography*, **43**(8), 1589-1610, doi:10.1175/JPO-D-12-0173.1.

Eymard, L., A. Weill, D. Bourras, C. Guerin, P. Le Borgne, and J. M. Lefevre, 2003: Use of ship mean data for validating model and satellite flux fields during the FETCH

Accepted for publication in *Journal of Physical Oceanography*. DOI 10.1175/JPO-D-22-0156.1.

experiment. *Journal of Geophysical Research*, **108**(C3), 8060, doi:10.1029/2001JC001207.

Fairall, C. W., E. F. Bradley, D. P. Rogers, J. B. Edson, and G. S. Young, 1996: Bulk parameterization of air-sea fluxes for Tropical Ocean-Global Atmosphere Coupled-Ocean Atmosphere Response Experiment. *Journal of Geophysical Research*, **101**(C2), 3747-3764, doi:10.1029/95JC03205.

Feng, Z., and Coauthors, 2021: A global high-resolution mesoscale convective system database using satellite-derived cloud tops, surface precipitation, and tracking. *Journal of Geophysical Research: Atmospheres*, **126**, e2020JD034202, https://doi.org/10.1029/2020JD034202.

Garg, P., S. W. Nesbitt, T. J. Lang, and G. Priftis, 2021: Diurnal cycle of tropical oceanic mesoscale cold pools. *Journal of Climate*, **34**(23), 9305-9326, doi:10.1175/JCLI-D-20-0909.1.

Gelaro, R., and Coauthors, 2017: The Modern-Era Retrospective Analysis for Research and Applications, version 2 (MERRA-2). *Journal of Climate*, **30**(14), 5419-5454, doi:10.1175/JCLI-D-16-0758.1.

Giglio, D., S. T. Gille, A. C. Subramanian, and S. Nguyen, 2017: The role of wind gusts in upper ocean diurnal variability. *Journal of Geophysical Research: Oceans*, **122**(9), 7751-7764, doi:10.1002/2017JC012794.

Giglio, D., S. T. Gille, B. D. Cornuelle, A. C. Subramanian, F. J. Turk, S. Hristova-Veleva, and D. Northcott, 2022: Annual Modulation of Diurnal Winds in the Tropical Oceans. *Remote Sensing*, **14**(3), 459, doi:10.3390/rs14030459.

Gill, A. E., 1982: *Atmosphere-Ocean Dynamics*. 662 pp., Academic, London.

Godfrey, J. S., and A. C. M. Beljaars, 1991: On the turbulent fluxes of buoyancy, heat and moisture at the air-sea interface at low wind speeds. *Journal of Geophysical Research*, **96**(C12), 22043-22048, doi:10.1029/91JC02015.

Hersbach, H., and Coauthors, 2020: The ERA5 global reanalysis. *Quarterly Journal of the Royal Meteorological Society*, **146**, 1999-2049, doi:10.1002/qj.3803.

Accepted for publication in *Journal of Physical Oceanography*. DOI 10.1175/JPO-D-22-0156.1.

Hourdin, F., and Coauthors, 2020: LMDZ6A: The atmospheric component of the IPSL climate model with improved and better tuned physics. *Journal of Advances in Modeling Earth Systems*, **12**(7), e2019MS001892, doi:10.1029/2019MS001892.

Joseph, J., M. S. Girishkumar, M. J. McPhaden, and E. Rao, 2021: Diurnal variability of atmospheric cold pool events and associated air-sea interactions in the Bay of Bengal during the summer monsoon. *Climate Dynamics*, **56**, 837-853, doi:10.1007/s00382-020-05506-w.

Klaver R., R. Haarsma, P. L. Vidale, and W. Hazeleger, 2020: Effective resolution in high resolution global atmospheric models for climate studies. *Atmospheric Science Letters*, 2020, 21:e952, https://doi.org/10.1002/asl.952.

Ledvina, D. V., G. S. Young, R. A. Miller, and C. W. Fairall, 1993: The effect of averaging on bulk estimates of heat and momentum fluxes for the tropical western Pacific Ocean. *Journal of Geophysical Research*, **98**(C11), 20211-20217, doi:10.1029/93JC01856.

Lee, T., and W. T. Liu, 2005: Effects of high-frequency wind sampling on simulated mixed layer depth and upper ocean temperature. *Journal of Geophysical Research*, **110**, C05002, doi:10.1029/2004JC002746.

Lin, X., X. M. Zhai, Z. Wang, and D. Munday, 2018: Mean, variability and trend of Southern Ocean wind stress: Role of wind fluctuations. *Journal of Climate*, **31**(9), 3557-3573, doi:10.1175/JCLI-D-17-0481.1.

Lin, X., X. M. Zhai, Z. Wang, and D. Munday, 2020: Southern Ocean Wind Stress in CMIP5 Models: Role of Wind Fluctuations. *Journal of Climate*, **33**(4), 1209-1226, doi:10.1175/JCLI-D-19-0466.1.

Masich, J., W. S. Kessler, M. F. Cronin, and K. R. Grissom, 2021: Diurnal cycles of near-surface currents across the tropical Pacific. *Journal of Geophysical Research: Oceans*, **126**(4), e2020JC016982, doi:10.1029/2020JC016982.

McPhaden, M. J., and Coauthors, 2010: The global tropical moored buoy array, OceanObs09 Community White Paper, Venice, Italy.

Accepted for publication in *Journal of Physical Oceanography*. DOI 10.1175/JPO-D-22-0156.1.

Ouni, M., A. Mehra, and A. Harzallah, 2021: The effect of the temporal resolution of the wind forcing on a central Mediterranean Sea model. *Dynamics of Atmospheres and Oceans*, **96**, 101262, doi:10.1016/j.dynatmoce.2021.101262.

Ponte, R. M., and R. D. Rosen, 2004: Nonlinear effects of variable winds on ocean stress climatologies. *Journal of Climate*, **17**(6), 1283-1293, doi:10.1175/1520-0442(2004)017<1283:NEOVWO>2.0.CO;2.

Praveen Kumar, B., J. Vialard, M. Lengaigne, V. Murty, and M. J. McPhaden, 2012: Tropflux: air-sea fluxes for the global tropical oceans-description and evaluation. *Climate dynamics*, **38**, 1521-1543, doi:10.1007/s00382-011-1115-0.

Praveen Kumar, B., J. Vialard, M. Lengaigne, V. Murty, M. J. McPhaden, M. F. Cronin, F. Pinsard, and K. Gopala Reddy, 2013: Tropflux wind stresses over the tropical oceans: evaluation and comparison with other products. *Climate Dynamics*, **40**, 2049-2071, doi:10.1007/s00382-012-1455-4.

Redelsperger, J. L., F. Guichard, and S. Mondon, 2000: A parameterization of mesoscale enhancement of surface fluxes for large-scale models. *Journal of Climate*, **13**(2), 402-421, doi:10.1175/1520-0442(2000)013<0402:APOMEO>2.0.CO;2.

Risien, C.M., and D.B. Chelton, 2008: A Global Climatology of Surface Wind and Wind Stress Fields from Eight Years of QuikSCAT Scatterometer Data. *J. Phys. Oceanogr.*, 38, 2379-2413, doi:10.1175/2008JPO3881.1.

Skamarock, W. C., 2004: Evaluating mesoscale NWP models using kinetic energy spectra. *Monthly Weather Review*, 132, 3019-3032, https://doi.org/10.1175/MWR2830.1.

Serra, Y. L., M. F. Cronin, and G. N. Kiladis, 2007: Sub-seasonal variance of surface meteorological parameters in buoy observations and reanalyses. *Geophysical Research Letters*, **34**(12), 237-254, doi:10.1029/2007GL029506.

Takahashi, K., 2012: Thermotidal and land-heating forcing of the diurnal cycle of oceanic surface winds in the eastern tropical Pacific. *Geophysical Research Letters*, **39**, L04805, doi:10.1029/2011GL050692.

Accepted for publication in *Journal of Physical Oceanography*. DOI 10.1175/JPO-D-22-0156.1.

Thushara, V., and P. N. Vinayachandran, 2014: Impact of diurnal forcing on intraseasonal sea surface temperature oscillations in the Bay of Bengal. *Journal of Geophysical Research: Oceans*, **119**(12), 8221-8241, doi:10.1002/2013JC009746.

Turk, F. J., S. Hristovaveleva, and D. Giglio, 2021: Examination of the daily cycle wind vector modes of variability from the constellation of microwave scatterometers and radiometers. *Remote Sensing*, **13**(1), 141, doi:10.3390/rs13010141.

Ueyama, R., and C. Deser, 2008: A climatology of diurnal and semidiurnal surface wind variations over the tropical Pacific Ocean based on the tropical atmosphere ocean moored buoy array. *Journal of Climate*, **21**(4), 593-607, doi:10.1175/JCLI1666.1.

Wu, Y., X. M. Zhai, and Z. Wang, 2016: Impact of synoptic atmospheric forcing on the mean ocean circulation. *Journal of Climate*, **29**(16), 5709-5724, doi:10.1175/JCLI-D-15-0819.1.

Wu, Y., Z. Wang, C. Liu, and X. Lin, 2020: Impacts of High-Frequency Atmospheric Forcing on Southern Ocean Circulation and Antarctic Sea Ice. *Advances in Atmospheric Sciences*, **37**, 515-531, doi:10.1007/s00376-020-9203-x.

Wunsch, C., and R. Ferrari, 2004: Vertical mixing, energy, and the general circulation of the oceans. *Annual Review of Fluid Mechanics*, **36**, 281-314, doi:10.1146/annurev.fluid.36.050802.122121.

Yan, Y., L. Zhang, X. Song, G. Wang, and C. Chen, 2021: Diurnal variation in surface latent heat flux and the effect of diurnal variability on the climatological latent heat flux over the tropical oceans. *Journal of Physical Oceanography*, **51**(11), 3401-3415, doi:10.1175/JPO-D-21-0128.1.

Yan, Y., X. Song, G. Wang, and C. Chen, 2022: Importance of High-frequency (≤30-day) Wind Variability to the Annual Climatology of the Surface Latent Heat Flux Inferred from the Global Tropical Moored Buoy Array. *Journal of Geophysical Research: Oceans*, **127**(3), e2021JC018094, doi:10.1029/2021JC018094.

Yu, Y., S. H. Chen, Y. H. Tseng, X. Guo, and H. Gao, 2020: Importance of diurnal forcing on the summer salinity variability in the East China Sea. *Journal of Physical Oceanography*, **50**(3), 633-653, doi:10.1175/JPO-D-19-0200.1.

Accepted for publication in *Journal of Physical Oceanography*. DOI 10.1175/JPO-D-22-0156.1.

Yuan, J., and R. A. Houze, 2010: Global variability of mesoscale convective system anvil structure from A-train satellite data. *Journal of Climate*, **23**(21), 5864-5888, https://doi.org/10.1175/2010JCLI3671.1.

Zeng, X. B., Q. Zhang, D. Johnson, and W. K. Tao, 2002: Parameterization of wind gustiness for the computation of ocean surface fluxes at different spatial scales. *Monthly Weather Review*, **130**(8), 2125-2133, doi:10.1175/1520-493(2002)130<2125:POWGFT>2.0.CO;2.

Zhai, X. M., 2013: On the wind mechanical forcing of the ocean general circulation. *Journal of Geophysical Research: Oceans*, **118**(12), 6561-6577, doi:10.1002/2013JC009086.

Zhai, X. M., and C. Wunsch, 2013: On the variability of wind power input to the oceans with a focus on the subpolar North Atlantic. *Journal of Climate*, **26**(11), 3892-3903, doi:10.1175/JCLI-D-12-00472.1.

Zhai, X. M., H. L. Johnson, D. P. Marshall, and C. Wunsch, 2012: On the wind power input to the ocean general circulation. *Journal of Physical Oceanography*, **42**(8), 1357-1365, doi:10.1175/JPO-D-12-09.1.

Zhou, S., X. M. Zhai, and I. A. Renfrew, 2018: The impact of high-frequency weather systems on SST and surface mixed layer in the central Arabian Sea. *Journal of Geophysical Research: Oceans*, **123**(2), 1091-1104, doi:10.1002/2017JC013609.

Accepted for publication in *Journal of Physical Oceanography*. DOI 10.1175/JPO-D-22-0156.1.